

Friction drag reduction achievable by near-wall turbulence manipulation at high Reynolds numbers

Kaoru Iwamoto,* Koji Fukagata, Nobuhide Kasagi, and Yuji Suzuki

Department of Mechanical Engineering, The University of Tokyo,

7-3-1 Hongo, Bunkyo-ku, Tokyo 113-8656, Japan

(Dated: Received 16 August 2004; accepted 29 September 2004)

Abstract

The Reynolds-number dependence of the drag reduction achievable by diminishing to zero the near-wall turbulent velocity fluctuations is clarified. This reduction could be obtained by a virtual active feedback control system. The formula derived suggests that large drag reduction can be attained even at high Reynolds numbers if turbulence fluctuations adjacent to the wall are completely damped. For example, 35% drag reduction rate can be obtained at $Re_\tau = 10^5$ if the turbulence only below $y^+ = 10$ vanishes. Thus, the active feedback control strategy, which has been studied mostly at low Reynolds numbers, would be much promising even in high Reynolds number flows of real applications. Results from the direct numerical simulation of turbulent channel flow at a Reynolds number of $Re_\tau = 642$ are also presented to clarify the phenomena in the controlled flow. [DOI: 10.1063/1.1827276]

PACS numbers: 47.27.Eq, 47.27.Jv, 47.27.Nz, 47.27.Rc, 47.62.+q, 47.11.+j, 47.20.-k, 47.60.+i

* Author to whom correspondence should be addressed. Electronic mail: iwamoto@thtlab.t.u-tokyo.ac.jp

Turbulence control techniques for drag reduction and heat transfer augmentation are of great importance from the viewpoint of energy saving and environmental impact mitigation. Among various methodologies, active feedback control schemes attract much attention because of their potential of large control effect with small power input [1–3]. The pioneering studies [4–6] have shown through their direct numerical simulation (DNS) of turbulent channel flow that the skin friction drag can be substantially reduced by a small amount of local blowing/suction on the wall.

However, the Reynolds numbers assumed in most previous studies are $Re_\tau = 100 - 180$ (hereafter, Re_τ denotes the friction Reynolds number defined based on the wall friction velocity u_τ , the channel half-width δ , and the kinematic viscosity ν), where significant low-Reynolds-number effects must exist. Actually, Iwamoto *et al.* [7] showed in their DNS at $Re_\tau < 642$ that the performance of the suboptimal control [5] is gradually deteriorated as the Reynolds number is increased. The Reynolds numbers in real applications are far beyond the values of current DNS. For example, the friction Reynolds number of a Boeing 747 aircraft is roughly estimated to be $Re_\tau \sim 10^5$ under a typical cruising condition. For flows of such high Reynolds numbers, where highly complex turbulent structures exist with a very wide range of turbulent spectra, no quantitative knowledge is available on the effectiveness of active feedback control.

According to the analytical relation between the Reynolds shear stress distribution and the skin friction coefficient [8], the amount of drag reduction depends on the degree of Reynolds stress suppression not only in the near-wall layer, but also away from the wall. As the Reynolds number increases, the contribution of the region away from the wall becomes dominant [7]. On the other hand, the basic strategy of the active feedback control using sensors and actuators distributed on the wall is to selectively manipulate the turbulence regeneration mechanism and suppress the turbulence intensity in the near-wall layer. Therefore, it is not straightforward to expect that the active feedback control scheme tested at low Reynolds numbers should also be effective at much higher Reynolds numbers.

In the present study, we theoretically investigate the Reynolds number effect on the drag reduction rate achieved by an active feedback control acting only on the near-wall layer. We assume ideally that all velocity fluctuations in the near-wall layer, i.e., $0 \leq y \leq y_d$, are perfectly damped by the active feedback control, and derive a formula of the relationship between the Reynolds number, the thickness of the damping layer y_d , and the drag reduction rate.

We assume a fully developed turbulent channel flow of a constant flow rate. The friction coefficient in the uncontrolled flow is defined as $C_f \equiv \tau_w / ((1/2)\rho U_m^2)$, where τ_w is the wall shear

stress, ρ is the density, and U_m is the bulk mean velocity. The drag reduction rate is defined as $R_D \equiv (C_f - C'_f)/C_f$, where the single prime denotes quantities of the controlled flow. Under the constant flow rate condition, the wall shear stress τ'_w , and the wall friction velocity u'_τ of the controlled flow are given by

$$\tau'_w = (1 - R_D)\tau_w, \quad u'_\tau = \sqrt{1 - R_D} u_\tau. \quad (1)$$

Because the velocity fluctuations are assumed to be perfectly suppressed in the damped layer, no Reynolds shear stress arises while the total shear stress is equal to the viscous shear stress in the region of $0 \leq y \leq y_d$. Thus, the shear stress τ'_d and the friction velocity $u'_{\tau d}$ at the upper boundary of the damped layer ($y = y_d$) are given by

$$\tau'_d = \left(1 - \frac{y_d}{\delta}\right)\tau'_w, \quad u'_{\tau d} = \sqrt{\left(1 - \frac{y_d}{\delta}\right)} u'_\tau, \quad (2)$$

where δ is the channel half-width, and the subscript of d denotes quantities at $y = y_d$.

Figure 1 shows the mean velocity profiles of the uncontrolled and controlled flows. The mean velocity profile in the damped layer is that of a laminar flow with the wall shear stress τ'_w . Any velocity fluctuations are absent at $y = y_d$ and $y = 2\delta - y_d$. Therefore, when viewed from the frame moving at the mean velocity at $y = y_d$, i.e., $U = U'_d$, the flow in the undamped layer (i.e., $y_d \leq y \leq 2\delta - y_d$) is identical to an ordinary (i.e., uncontrolled) turbulent channel flow with the channel width of $2(\delta - y_d)$, the effective bulk mean velocity of $U'_{m \text{ eff}}$, and the “wall” shear stress of τ'_d . Since the flow rate is kept constant, the bulk mean velocity U_m is expressed by

$$U_m = \frac{1}{\delta} \int_0^{y_d} U dy + U'_d \cdot \left(1 - \frac{y_d}{\delta}\right) + U'_{m \text{ eff}} \cdot \left(1 - \frac{y_d}{\delta}\right). \quad (3)$$

Three terms on the right-hand side (RHS) represent, in the order of appearance, contributions from the damped layer, the inertial part with the velocity of U'_d , and the turbulent flow in a reduced-size channel with an effective bulk mean velocity of $U'_{m \text{ eff}}$, respectively.

In the following, we transform each term in Eq. (3) as a function of u_τ . The laminar velocity profile in the damped layer is given by

$$U = \frac{\tau'_w}{\mu} y \left(1 - \frac{y}{2\delta}\right), \quad (4)$$

where μ denotes the viscosity. Integration of Eq. (4) gives the first term on the RHS of Eq. (3) as

$$\frac{1}{\delta} \int_0^{y_d} U dy = \frac{1}{2} \left(\frac{y_d}{\delta}\right)^2 \left(1 - \frac{y_d}{3\delta}\right) (1 - R_D) Re_\tau \cdot u_\tau, \quad (5)$$

where Eq. (1) is used to substitute τ'_w .

The mean velocity U'_d at $y = y_d$ is given by Eq. (4) as

$$U'_d = \frac{\tau'_w}{\mu} y_d \left(1 - \frac{y_d}{2\delta}\right). \quad (6)$$

Thus, the second term on the RHS of Eq. (3) can be expressed, by using Eqs. (1) and (6), as

$$\begin{aligned} U'_d \cdot \left(1 - \frac{y_d}{\delta}\right) = \\ \frac{y_d}{\delta} \left(1 - \frac{y_d}{2\delta}\right) \left(1 - \frac{y_d}{\delta}\right) (1 - R_D) Re_\tau \cdot u_\tau. \end{aligned} \quad (7)$$

Dean's formula [9] derived from the logarithmic law is adopted to describe the relationship between the bulk mean velocity U_m and the wall friction velocity u_τ , i.e.,

$$U_m = \left(\frac{1}{\kappa} \ln Re_\tau + F\right) u_\tau, \quad \kappa = 0.41, \quad F = 3.2. \quad (8)$$

Substitution of Eqs. (2) and (8) (which stands for the narrowed channel flow with $U'_{m \text{ eff}}$) into the third term on the RHS of Eq. (3) results in

$$\begin{aligned} U'_{m \text{ eff}} \cdot \left(1 - \frac{y_d}{\delta}\right) = \left(1 - \frac{y_d}{\delta}\right)^{\frac{3}{2}} (1 - R_D)^{\frac{1}{2}} \times \\ \left[\frac{1}{\kappa} \ln \left\{ \left(1 - \frac{y_d}{\delta}\right)^{\frac{3}{2}} (1 - R_D)^{\frac{1}{2}} Re_\tau \right\} + F\right] \cdot u_\tau. \end{aligned} \quad (9)$$

Finally, by collecting these expressions, i.e., Eqs. (5) and (7)-(9), we obtain the following identity equation:

$$\begin{aligned} \frac{1}{\kappa} \ln Re_\tau + F = \frac{y_d}{\delta} \left(1 - \frac{y_d}{\delta} + \frac{1}{3} \frac{y_d^2}{\delta^2}\right) (1 - R_D) Re_\tau + \\ \left(1 - \frac{y_d}{\delta}\right)^{\frac{3}{2}} (1 - R_D)^{\frac{1}{2}} \times \\ \left[\frac{1}{\kappa} \ln \left\{ \left(1 - \frac{y_d}{\delta}\right)^{\frac{3}{2}} (1 - R_D)^{\frac{1}{2}} Re_\tau \right\} + F\right], \end{aligned} \quad (10)$$

with the Reynolds number of the uncontrolled flow Re_τ , the thickness of damping layer divided by channel half-width y_d/δ , and the drag reduction rate R_D . Thus, R_D can be calculated for given Re_τ and y_d/δ . The accuracy of Eq. (10) at a sufficiently wide Reynolds number range ($10^3 < Re_\tau < 5 \cdot 10^5$) is verified by the good agreement between the sole empirical formula used in the derivation above, i.e., Eq. (8), and the experimental data [9, 10].

Figure 2(a) shows the dependency of R_D on Re_τ for constant values of y_d^+ . Hereafter, all variables with the superscript of + are those nondimensionalized by the wall friction velocity of the

uncontrolled flow u_τ , and the kinematic viscosity ν . As Re_τ increases, R_D decreases. The Reynolds number dependency of R_D , however, is found to be weak. For $y_d^+ = 10$, for instance, the drag reduction rate R_D is about 0.43 (i.e., 43% drag reduction) at $Re_\tau = 10^3$, and about 35% even at $Re_\tau = 10^5$. The damping layer at $Re_\tau = 10^5$ is extremely thin as compared to the channel half width, i.e., $y_d/\delta = 10^{-4}$.

Figure 2(b) shows the Reynolds number dependency of y_d^+ required to achieve a specified drag reduction rate R_D . As Re_τ increases, y_d^+ gradually increases. Equation (10) reduces for high Reynolds numbers, where $y_d/\delta \ll 1$ holds, to $y_d^+ \sim \ln Re_\tau$. Namely, the Reynolds number dependency is very weak. This asymptotic relation is in good agreement with Eq. (10) for $Re_\tau > 4 \times 10^3$, as shown in Fig. 2(b). Thus, large drag reduction can be obtained even at high Reynolds numbers only by damping the near-wall velocity fluctuations.

It is worth noting that an equation similar to Eq. (10) can be obtained by using another Dean's formula derived from the power law. This gives slight quantitative difference in the resulting R_D ($R_D = 30\%$ at $Re_\tau = 10^5$ and $y_d^+ = 10$) and y_d^+ ($y_d^+ = 16$ at $Re_\tau = 10^5$ and $R_D = 40\%$), but the trend is essentially similar to Fig. 2.

The mechanism of drag reduction is examined in detail by DNS of turbulent channel flow at a moderate Reynolds number [7]. The Navier-Stokes equation is solved under a constant flow rate at a Reynolds number of $Re_\tau = 642$, i.e.,

$$\frac{\partial u_i^+}{\partial t^+} + u_j^+ \frac{\partial u_i^+}{\partial x_j^+} = -\frac{\partial p'^+}{\partial x_i^+} + \frac{\partial^2 u_i^+}{\partial x_j^+ \partial x_j^+} - \frac{1}{\phi^+} f(y^+) u_i^+, \quad (11)$$

where the third term on the RHS is the damping term and $f(y)$ is defined as

$$f(0 \leq y^+ \leq y_d^+) = 1, \quad f(y^+ > y_d^+) = 0. \quad (12)$$

It is assumed that numerous remote sensors acquire the velocity information in the near-wall thin layer and that based on the sensor signals local body force is imposed to diminish any velocity fluctuation in that region. The thickness of damping layer is changed as $y_d^+ = 30$ and 60. We employ the damping time constant of $\phi^+ = 1$ to mimic strong damping force near both the walls. Hereafter, u , v , and w denote the velocity components in the streamwise (x), wall-normal (y), and spanwise (z) directions, respectively. Figure 3 shows contours of the instantaneous streamwise velocity fluctuation u' in a cross-stream plane. Velocity fluctuations in the damped layer are almost zero as shown in Figs. 3 (b) and 3 (c). The effective Reynolds number in the undamped region, defined by $Re'_{\tau \text{ eff}} \equiv u'_{\tau d}(\delta - y_d)/\nu$, is decreased with increasing the thickness of damping layer, so

that the fine-scale turbulent structures with $y_d^+ = 60$ are more suppressed than those with $y_d^+ = 30$. The drag reduction rates are $R_D \approx 60$ and 74% for $y_d^+ = 30$ and 60 , respectively, which are in good agreement with the analytical values of 66 and 78% given by Eq. (10), respectively. Note that the small quantitative difference of R_D between the theory and the DNS results is attributed to the degree (or perfectness) of damping in the region of $0 \leq y \leq y_d$. As shown below, the velocity fluctuations slightly remain in the DNS, whereas those are assumed zero in the theoretical analysis.

Figure 4 shows the root-mean-square velocity fluctuations and the Reynolds shear stress with and without velocity fluctuation damping at $y^+ \leq 60$. These quantities are drastically decreased in the damping layer and also in the undamped region. This change in the Reynolds shear stress gives a clue on the large drag reduction mechanism if we use the decomposition of the skin friction drag proposed by Fukagata *et al.* [8], which reads

$$\tau_w^+ = \frac{3 Re_b}{2 Re_\tau^2} + \frac{1}{\delta} \int_0^\delta 3 \left(1 - \frac{y}{\delta}\right) (-\overline{u'^+ v'^+}) dy \quad (13)$$

in the wall unit of the uncontrolled flow. The first term on the RHS is the contribution of the laminar flow, while the second term is that of the turbulence, which is a weighted integral of the Reynolds shear stress distribution. In Fig. 4(b), the weighted Reynolds shear stress $3(1 - y/\delta)(-\overline{u'^+ v'^+})$ is also shown. As is noticed from Eq. (13), the difference in the areas surrounded by these two (uncontrolled and damped) curves of the weighted Reynolds stress directly corresponds to the drag reduction rate, i.e., $R_D = S(0 \leq y/\delta \leq 1) = 0.74$, where $S(\cdot)$ denotes the area. The area $S(0 \leq y^+ \leq 60)$ in the damping layer is 0.18 , and that in the undamped region is $S(y^+ \geq 60) = 0.56$. Namely, the drag reduction rate directly caused by the decrease of $(-\overline{u'^+ v'^+})$ in the near-wall damping layer is 18% , while the drag reduction rate due to the accompanied decrease of $(-\overline{u'^+ v'^+})$ in the undamped region is 56% . At higher Reynolds numbers, the relative thickness of the damping layer y_d/δ becomes smaller so that the contribution outside the damped layer should be dominant. Thus, large drag reduction by the wall control at high Reynolds numbers is mainly attributed to the decrease of the Reynolds stress in the region away from the wall.

Note that the near-wall-layer laminarization does not provide the maximum drag reduction. As is noticed from Eq. (13), we can get a drag reduction larger than that of relaminarization if the Reynolds shear stress $(-\overline{u'v'})$ becomes negative. Whether such a sublaminal drag can be achieved or not is still an open question (see, e.g., Bewley and Aamo [11]).

In summary, we derived a formula to describe the relationship between the Reynolds number and the drag reduction rate in turbulent channel flows, i.e., Eq. (10), by assuming ideal damping

of the velocity fluctuations in the near-wall layer. The derived formula as well as the following analysis by DNS indicates that large drag reduction can be attained even at high Reynolds numbers by damping the turbulence only near the wall, viz., without any direct manipulation of large-scale structures away from the wall. Therefore, the basic strategy behind the existing control schemes, i.e., attenuation of the near-wall turbulence, is also valid at high Reynolds numbers in real applications.

Acknowledgments

This work was supported through the Project for Organized Research Combination System by the Ministry of Education, Culture, Sports and Technology of Japan (MEXT).

References

- [1] P. Moin and T. Bewley, "Feedback control of turbulence," *Appl. Mech. Rev.* **47**, S3 (1994).
- [2] M. Gad-el-Hak, "Modern developments in flow control," *Appl. Mech. Rev.* **49**, 365 (1996).
- [3] N. Kasagi, "Progress in direct numerical simulation of turbulent transport and its control," *Int. J. Heat Fluid Flow* **19**, 125 (1998).
- [4] H. Choi, P. Moin, and J. Kim, "Active turbulence control for drag reduction in wall-bounded flows," *J. Fluid Mech.* **262**, 75 (1994).
- [5] C. Lee, J. Kim, and H. Choi, "Suboptimal control of turbulent channel flow for drag reduction," *J. Fluid Mech.* **358**, 245 (1998).
- [6] T. R. Bewley, P. Moin, and R. Temam, "DNS-based predictive control of turbulence: An optimal benchmark for feedback algorithms," *J. Fluid Mech.* **447**, 179 (2001).
- [7] K. Iwamoto, Y. Suzuki, and N. Kasagi, "Reynolds number effect on wall turbulence: Toward effective feedback control," *Int. J. Heat Fluid Flow* **23**, 678 (2002).
- [8] K. Fukagata, K. Iwamoto, and N. Kasagi, "Contribution of Reynolds stress distribution to the skin friction in wall-bounded flows," *Phys. Fluids* **14**, L73 (2002).
- [9] R. B. Dean, "Reynolds number dependence of skin friction and other bulk flow variables in two-dimensional rectangular duct flow," *ASME Trans. J. Fluids Eng.* **100**, 215 (1978).
- [10] M. V. Zagarola and A. J. Smits, "Mean-flow scaling of turbulent pipe flow," *J. Fluid Mech.* **373**, 33 (1998).
- [11] T. R. Bewley and O. M. Aamo, "A 'win-win' mechanism for low-drag transients in controlled two-dimensional channel flow and its implications for sustained drag reduction," *J. Fluid Mech.* **499**, 183 (2004).

List of Figures

- 1 Schematic mean velocity profiles. (a) Uncontrolled; (b) with damping in the near-wall layer.
- 2 (a) Dependency of the drag reduction rate R_D on the Reynolds number Re_τ with specified thicknesses of damping layer y_d^+ . (b) Thickness of the damping layer y_d^+ required to achieve specified drag reduction rates R_D .
- 3 Cross-sectional view of instantaneous velocity field at $Re_\tau \approx 642$. (a) Uncontrolled; (b) with damping at $y^+ \leq 30$; (c) with damping at $y^+ \leq 60$. Contours of the streamwise velocity fluctuation (white to black, $u'^+ = -1$ to $u'^+ = 1$).
- 4 (a) RMS velocity fluctuations. (b) Raw and weighted Reynolds shear stresses. Both are nondimensionalized by the friction velocity of the uncontrolled flow u_τ .

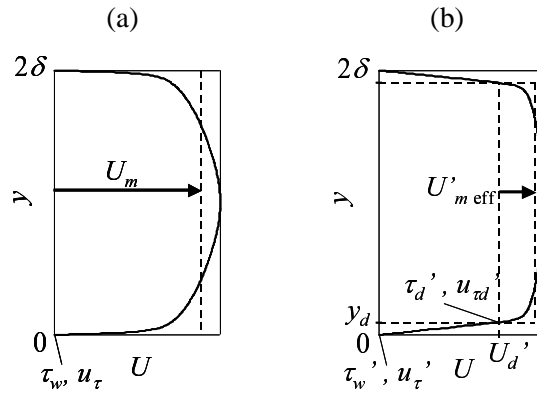


FIG. 1: Schematic mean velocity profiles. (a) Uncontrolled; (b) with damping in the near-wall layer.

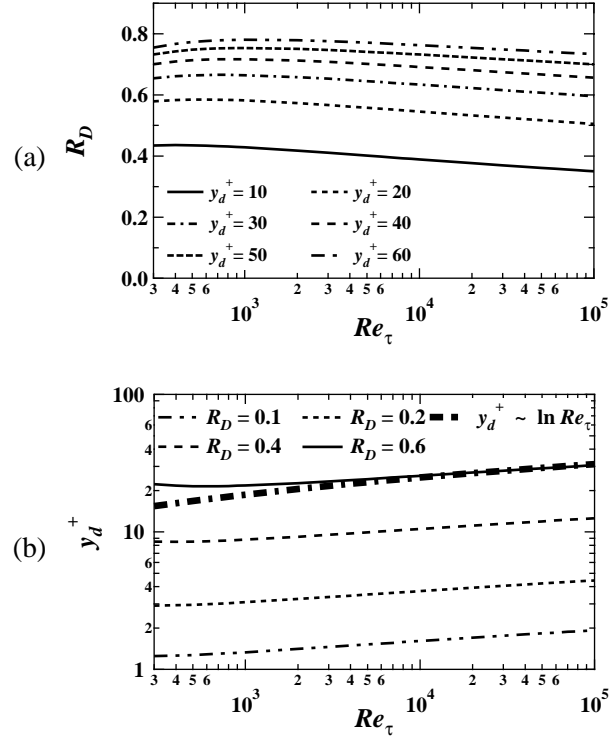


FIG. 2: (a) Dependency of the drag reduction rate R_D on the Reynolds number Re_τ with specified thicknesses of damping layer y_d^+ . (b) Thickness of the damping layer y_d^+ required to achieve specified drag reduction rates R_D .

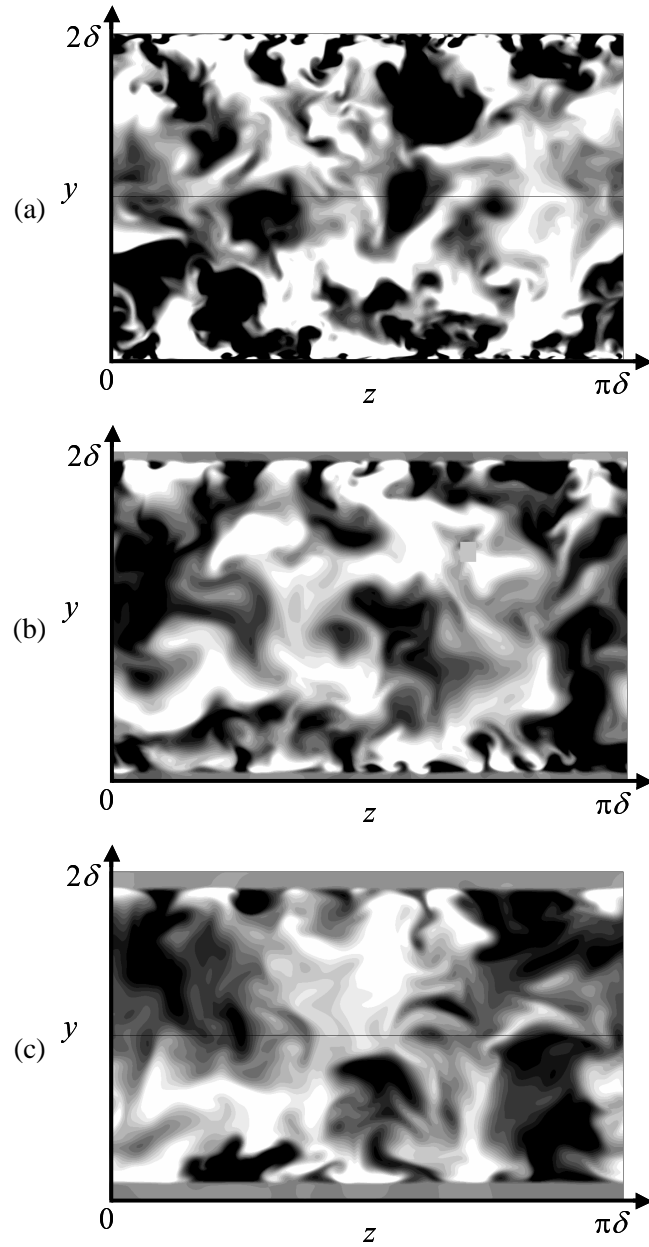


FIG. 3: Cross-sectional view of instantaneous velocity field at $Re_\tau \approx 642$. (a) Uncontrolled; (b) with damping at $y^+ \leq 30$; (c) with damping at $y^+ \leq 60$. Contours of the streamwise velocity fluctuation (white to black, $u'^+ = -1$ to $u'^+ = 1$).

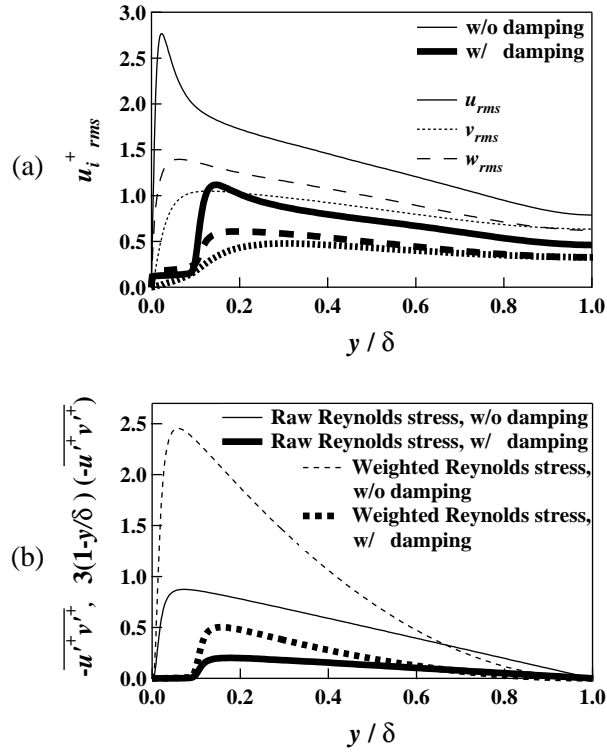


FIG. 4: (a) RMS velocity fluctuations without and with damping velocity fluctuations at $y^+ \leq 60$. (b) Raw and weighted Reynolds shear stresses. Both are nondimensionalized by the friction velocity of the uncontrolled flow u_τ .